Inorganica Chimica Acta 406 (2013) 1–9

Contents lists available at SciVerse ScienceDirect

Inorganica Chimica Acta

journal homepage: www.elsevier.com/locate/ica

Heterogenization of three homogeneous catalysts: A comparative study as epoxidation catalyst

Jaydeep Adhikary [a], Averi Guha [a], Tanmay Chattopadhyay [b,*], Debasis Das [a,*]

[a] Department of Chemistry, University of Calcutta, 92, A. P. C. Road, Kolkata 700009, India
[b] Department of Chemistry, Panchakot Mahavidyalaya, Sarbari, Purulia 723121, India

ARTICLE INFO

Article history:
Received 10 May 2013
Received in revised form 26 June 2013
Accepted 27 June 2013
Available online 5 July 2013

Keywords:
Homogeneous catalysts
Heterogenization
Modified MCM-41
Alkene epoxidation

ABSTRACT

Three homogeneous catalysts, $MnL^1Cl{\cdot}2H_2O(1.2\ H_2O)$ (HmC-1), $FeL^1(NO_3){\cdot}3H_2O$ (HmC-2) and $CoL^1(NO_3){\cdot}{\cdot}2H_2O$ (HmC-3) [L^1 = *N*,*N*′-ethylenebis(3-formyl-5-methylsalicylaldimine)] have been synthesized and characterized. The catalytic activity of HmC-1, -2 and -3 for epoxidation of alkenes has been investigated in the presence of terminal oxidant *tert*-butyl hydrogen peroxide (TBHP), in two solvents CH_3CN and CH_2Cl_2. Epoxidation of alkenes catalyzed by HmC-2 and HmC-3 in two solvents CH_3CN and CH_2Cl_2, have also been investigated with of iodosylbenzene (PhIO) as terminal oxidant. The epoxidation study with HmC-1 as catalyst was reported earlier using PhIO as oxidant. Highly ordered 2D-hexagonal mesoporous silica has been functionalized with 3-aminopropyltriethoxysilane (3-APTES) and this has been used to heterogenize the three synthesized homogeneous catalysts and thereby obtained three new heterogeneous catalysts HtC-1, HtC-2 and HtC-3. The heterogeneous catalysts have been characterized by FT-IR, solid state UV–Vis spectroscopy, powder X-ray diffraction (XRD) and scanning electron microscopy (SEM). The catalytic activity of these heterogeneous catalysts [HtC-(1-3)] for epoxidation of alkenes has been investigated in the presence of two terminal oxidants PhIO and TBHP, in two solvents CH_3CN and CH_2Cl_2 under mild conditions and compared their activity with their homogeneous counterpart.

1. Introduction

Catalytic epoxidation of olefins is an important synthetic method for both industry and academics [1]. Both homogeneous as well as heterogeneous catalytic systems are in use for that purpose. Transition metal complexes of salen type ligands are the most widely used homogeneous catalysts for epoxidation of olefins [2–4]. Usually, the product yields in homogenous catalytic reactions are very high because all the catalytic active sites are accessible, but the difficulty in separation of the catalyst and reaction products limits their scope. Heterogeneous catalysts appear to be a solution to this issue [5–7], because they have various attractive features such as easy product separation and catalyst recovery. So the heterogenization of homogeneous catalysts constitutes an interesting research area [8–13]. Various types of heterogenized catalysts are the metal complexes immobilized into solid supports such as molecular sieves [9,10], ion-exchange resins [11], polymer membrane [12], zeolite [14], and organic nanotubes [15] etc. Such immobilization often lowers the reactivity of these catalytic systems than that of homogenous catalysts due to the lower availability of active sites during the catalytic reactions. For instance, although a handful of heterogenized catalysts developed for epoxidation of unfunctionalized alkenes are in literature [16–23], most of them exhibit considerably lower activity [16–21] than their homogeneous counterparts. Beside this, heterogeneous catalysts sometime require high energy processes and drastic synthetic conditions for their preparation. So search for the new heterogenization method is crucial. Che et al. in 1999 reported [13] heterogenization of a homogeneous Cr(III)-Schiff-base catalyst via immobilizing on a modified MCM-41. They made co-ordinately unsaturated Cr(III)-Schiff-base complexes and took modified MCM-41 having terminal NH_2 group on the surface. Heretogenization was done through coordination of the chromium ion to the terminal NH_2 group of the surface-bound tether *via* simple addition or ligand substitution reactions. Recently Bhaumik et al. reported [24] another interesting way to produce immobilized Schiff-base ligand complexes of Ni(II) and Cu(II). They first of all functionalized highly ordered 2D-hexagonal mesoporous silica with 3-aminopropyltriethoxysilane (3-APTES) and then condensed it with a dialdehyde, 2,6-diformyl-4-methylphenol. The material thus obtained was separately treated with methanolic solution of copper(II) chloride and nickel(II) chloride to obtain copper and nickel anchored mesoporous materials, designated as Cu-AMM and Ni-AMM, respectively. However, the exact structures of the active sites of the heterogenized catalysts obtained following the above two methods seemed to be uncertain. In order to overcome

* Corresponding authors. Tel.: +91 9830345023.
E-mail address: dasdebasis2001@yahoo.com (D. Das).

0020-1693/$ - see front matter © 2013 Elsevier B.V. All rights reserved.
http://dx.doi.org/10.1016/j.ica.2013.06.045

that shortcoming here we introduce a new methodology to heterogenize homogenous catalysts. First of all we have synthesised Mn(III), Fe(III) and Co(III) complexes of a salen type ligand *N*,*N*′-ethylenebis(3-formyl-5-methylsalicylaldimine) (L^1) as homogeneous epoxidation catalyst where the salen ligand contains two uncoordinated formyl groups. Then heterogenization of these three structurally characterized homogeneous catalysts has been done following the steps as schematically represented in Scheme 1. The heterogenized catalysts thus obtained have been explored as epoxidation catalysts employing (*E*)-stilbene, styrene, cyclooctene and 1-octene as substrates in presence of *tert*-butyl hydrogen peroxide (TBHP) and PhIO as terminal oxidants in two solvents, acetonitrile and dichloromethane and their activities have been compared with their homogeneous counterpart. Here it is to note that syntheses of Mn complex and analogous complex of Fe with ClO_4^- as counter anion and some of their catalytic activity were reported earlier [25,26].

2. Experimental

2.1. Methods

Elemental analyses (carbon, hydrogen and nitrogen) were performed using a Perkin–Elmer 240 °C elemental analyzer. Infrared spectra (4000–500 cm^{-1}) were recorded at 27 °C using a Perkin–Elmer RXI FT-IR spectrophotometer with KBr pellets. Electronic spectra (800–200 nm) were obtained at 27 °C using a Shimadzu UV-3101PC with methanol as solvent and reference. The ^1H NMR spectra were recorded on a Bruker AC300 spectrometer. Magnetic susceptibilities were measured at 27 °C using an EG and G PAR 155 vibrating sample magnetometer with $Hg[Co(SCN)_4]$ as reference; diamagnetic corrections were made using Pascal's constants. Thermal analyses (TG–DTA) were carried out on a Mettler Toledo (TGA/SDTA851) thermal analyzer in flowing dinitrogen (flow rate: 30 cm^3 min^{-1}). The electrospray mass spectra were recorded on a MICROMASS Q-TOF mass spectrometer. The cyclic voltammetric measurements were carried out in dry acetonitrile solutions with 0.2 M TBAP as supporting electrolyte (scan rate = 10mV s^{-1}) employing a PAR potentiostat/galvanostat model Versa Stat-II. A three electrode system was used in which the counter and working electrodes were platinum foils and the reference electrode was a saturated calomel electrode. Field Emission Scanning Electron Microscope (FE-SEM) measurement was carried out with JEOL JSM-6700F field-emission microscope. X-ray powder diffraction (XRPD) was performed on a XPERT-PRO Diffractometer monochromated Cu Kα radiation (40.0 kV, 30.0 mA) at room temperature.

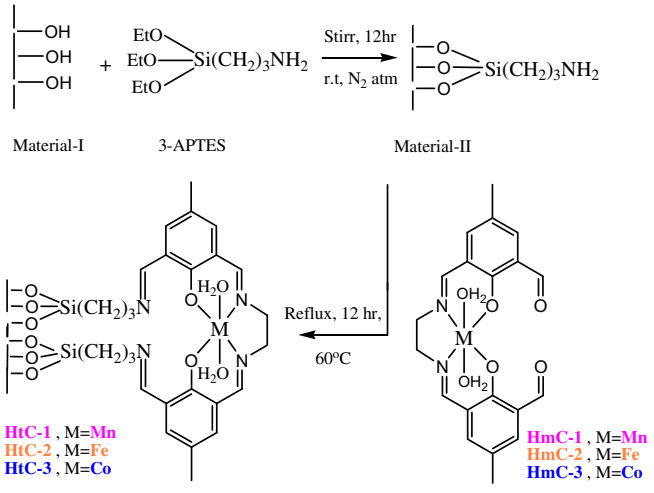

Scheme 1. Synthetic out-line of the catalysts.

2.2. Materials

All chemicals were obtained from commercial sources and used as received. Solvents were dried according to standard procedure and distilled prior to use. Styrene, (*E*)-stilbene, cyclooctene, 1-octene, *tert*-butyl hydrogen peroxide (TBHP) were purchased from Aldrich and used in epoxidation experiments without further purification. Polyethylene glycol dodecyl ether (Brij-35), tetramethylammoniumhydroxide (TMAOH) were purchased from Aldrich. 3-aminopropyltriethoxysilane (3-APTES), cetyl trimethyl ammonium bromide (CTAB) were purchased from Spectochem and Tartaric acid (TA) from Merck.

2.3. Preparation of the functionalized mesoporous material (M-II)

The functionalized mesoporous material (M-II) was prepared by following the reported method [27].

2.4. Synthesis of ligand (L^1) and homogenous catalysts

2, 6-Diformyl-4-methylphenol was prepared according to the literature method [28]. The Schiff-base *N*,*N*′-ethylenebis(3-formyl-5-methylsalicylaldimine) (L^1) was synthesized following the similar procedure as we reported earlier [25].

2.5. Synthesis of homogenous catalysts (HmC)

2.5.1. $MnL^1Cl{\cdot}2H_2O(1.2\ H_2O)$ (HmC-1)

HmC-1 was synthesized and characterized according to same procedure as reported earlier [25].

2.5.2. $FeL^1(NO_3){\cdot}3H_2O$ (HmC-2)

HmC-2 was synthesized by drop wise addition of an aqueous solution (20 mL) of $Fe(NO_3)_3{\cdot}6H_2O$ (0.404 g, 1 mmol) to a heated suspension of L^1(0.352 g,1 mmol) in ethanol (50 mL). A brown color developed immediately upon dissolution of the ligand. The solution was allowed to stir open to the atmosphere for 6 h. A clear deep brown solution was obtained. The solution was kept for crystallization. After a few days, brown crystals of HmC-2 (0.38 g, 75%) suitable for X-ray data collection were separated out. *Anal.* Calc. for $FeL^1(NO_3){\cdot}3H_2O$: C, 45.98; H, 4.59; N, 8.04. Found: C, 45.68; H, 4.60; N, 8.01%. IR (KBr): ν(C=O) 1656 cm^{-1}; ν(C=N) 1622 cm^{-1}; ν(skeletated vibration) 1544 cm^{-1} $\nu(H_2O)$ 3403 cm^{-1}; $\nu(NO_3^-)$ 1381. UV λ_{max} (MeOH)/nm 333, 501sh (ε/dm^3 mol^{-1} cm^{-1} 7100, 1137).

2.5.3. $CoL^1(NO_3){\cdot}2H_2O$ (HmC-3)

HmC-3 was synthesized by drop wise addition of an aqueous solution (20 mL) of $Co(NO_3)_2{\cdot}6H_2O$(0.291 g, 1 mmol) to a heated suspension of L^1(0.352 g, 1 mmol) in ethanol (50 mL). A reddish-brown color developed immediately upon dissolution of the ligand. The solution was allowed to stir open to the atmosphere for 6 h. A brown complex (0.41 g, 80%) thus precipitated was isolated by filtration, washed with water and dried in vacuum. *Anal.* Calc. for $CoL^1(NO_3){\cdot}2H_2O$: C, 47.33; H, 4.33; N, 8.28. Found: C, 47.32; H, 4.35; N, 8.30%. IR (KBr): ν(C=O) 1660.5 cm^{-1}; ν(C=N) 1624.9 cm^{-1}; $\nu(H_2O)$ 3330.8 cm^{-1}; ν(skeletated vibration) 1546.9 cm^{-1}; $\nu(NO_3^-)$ 1384.5 cm^{-1}. ^1H NMR (300 MHz, D_6-DMSO): δ 11.09 (2H, s, Ar–CHO), 8.36 (2H, s, –CH=N–), 7.66 (4H, s, Ar–H), 4.18 (4H, s, N–CH_2–CH_2–N), 2.04 (6H, s, Ar–CH_3). UV λ_{max} (MeOH)/nm 324, 410, 608sh (ε/$dm^3mol^{-1}cm^{-1}$ 22,000, 37500, 4000). TG analysis: 0.923 mg weight loss (7.22% of 12.77 mg complete: expected weight loss 7.1%) at 125 °C ESI-MS: m/z = 477.93 amu corresponds to $[CoL^1{\cdot}2H_2O + MeOH]^+$.

2.6. Synthesis of heterogeneous catalysts (HtC)

2.6.1. Mn-catalyst (HtC-1)

HtC-1 was synthesized by refluxing 2 g of M-II with 320 mg of HmC-1 in methanol (25 mL) for 12 h at 60 °C. The resulting brown solid was collected by filtration, repeatedly washed with hot methanol until the filtrate became colorless. Catalyst was finally dried in a vacuum desiccator. *Anal.* Calc. for HtC-1; IR (KBr): ν(C=N) 1638.2 cm^{-1}; $\nu(H_2O)$ 3427 cm^{-1}; ν(skeletated vibration) 1547.9 cm^{-1}. Solid UV (nm): 258, 281, 347, 428. TG analysis: 0.5369 mg weight loss (5.488% of 9.783 mg complex: expected weight loss 5.38%) at 100 °C.

2.6.2. Fe-catalyst (HtC-2)

HtC-2 was synthesized by refluxing 2 g of M-II and 320 mg of HmC-2 in 25 mL of methanol for 12 h at 60 °C. The resulting brown solid was collected by filtration, repeatedly washed with hot methanol until the filtrate became colorless. The solid product was red in color. For HtC-2; IR (KBr): ν(C=N) 1630.5 cm^{-1}; $\nu(H_2O)$ 3423 cm^{-1}; ν(skeletated vibration) 1545.6 cm^{-1}; $\nu(NO_3^-)$ 1382.7 cm^{-1}. Solid UV (nm): 258, 281, 345, 446, 530. TG analysis: 0.4339 mg weight loss (5.25% of 8.259 mg complex: expected weight loss 5.39%) at 98 °C.

2.6.3. Co-catalyst (HtC-3)

HtC-3 was prepared by refluxing 25 mL of methanolic solution of HmC-3(300 mg) and 2 g of M-II. The resulting brown solid was collected by filtration, repeatedly washed with hot methanol until the filtrate became colorless. The catalyst had light yellow color. For HtC-3; IR (KBr): ν(C=N) 1649.9 cm^{-1}; $\nu(H_2O)$ 3426 cm^{-1}; ν(skeletated vibration) 1542 cm^{-1}; $\nu(NO_3^-)$ 1388.9 cm^{-1}. Solid UV (nm): 259, 279, 346, 439, 645. TG analysis: 0.3304 mg weight loss (4.38% of 7.603 mg complex: expected weight loss 4.45%) at 101 °C.

2.7. Preparation of iodosylbenzene

It was prepared by hydrolysis of the corresponding diacetate with aqueous sodium hydroxide according to literature method [29]. In every epoxidation experiment freshly prepared PhIO was used.

2.8. Epoxidation study of catalysts

2.8.1. Epoxidation of alkenes catalyzed by HmC-(1-3)

To a solution of alkene (3 mmol) in acetonitrile or dichloromethane (50 mL), 0.1 mmol of HmC-(1-3) was added and then 70% TBHP (450 mg, 5 mmol) or PhIO (666 mg, 3 mmol) was added to that solution and the resultant mixture were stirred at room temperature for 2 h in air. Iodosylbenzene or TBHP was added portion wise to the solution. The reaction progress was monitored by TLC. After removal of solvent, the crude product was purified by flash chromatography. Identification of the epoxide was performed by ^{1}H NMR spectroscopy.

2.8.2. Epoxidation of alkenes catalyzed by HtC-(1-3)

To a solution of alkene (3 mmol) in acetonitrile or dichloromethane (50 mL), 200 mg of HtC-(1-3) was suspended and then 70% TBHP (360 mg, 4 mmol) or PhIO (666 mg, 3 mmol) was added and the resultant mixture were stirred at room temperature for 2 h in air. Here also we added iodosylbenzene or TBHP portion wise to the solution. The reaction progress was monitored by TLC. After completion of the reaction, the catalyst was filtered off and the solvent was removed by rotary evaporator. The crude product was thus obtained was purified by flash chromatography. Identification of the epoxide was performed by ^{1}H NMR spectroscopy.

2.9. X-ray data collection and structure determination

Diffraction data for HmC-2 was collected at room temperature (293 K) on a Bruker Smart CCD diffractometer equipped with graphite – monochromated Mo Kα radiation (λ = 0.71073 Å). Cell refinement, indexing and scaling of the data set were carried out using Bruker SMART APEX and Bruker SAINT package [30]. The structure was solved by direct methods and subsequent Fourier analyses [31] and refined by the full-matrix least-squares method based on F^2 with all observed reflections using SIR-92 and SHELX-97 [32], software. For the complex, all non-hydrogen atoms were refined with anisotropic thermal parameters and the hydrogen atoms were fixed at their respective positions riding on their carrier atoms and refined anisotropically. All the calculations were performed using the WinGX System, Ver 1.80.05 [33], PLATON99 [34], ORTEP3 [35] programs. Selected crystallographic data and refinement details are displayed in Table 1.

3. Results and discussion

3.1. Preparation and characterization of homogenous catalysts

The purposely selected salen-type Schiff-base ligand *N*,*N*′-ethylenebis(3-formyl-5-methylsalicylaldimine) (L^1) and its Mn(III) complex (HmC-1) have been prepared and identified by its reported physicochemical properties [25]. The newly synthesized Fe(III) complex, (HmC-2) exhibits very similar physicochemical properties as we observed earlier with an analogous complex having ClO_4^- as counter anion [26]. Earlier we failed to prepare single crystals of the Fe(III) complex but this time with NO_3^- as counter anion we are successful in getting single crystals suitable for X-ray analysis (*vide infra*). The composition of the HmC-3 has been assigned by elemental analyses. The solvent contents of HmC-3 are determined by thermogravimetric analysis. The HmC-3 exhibits characteristic IR bands at 1660, 1624 and 1546 cm^{-1} assigned to C=O, C=N and skeletal vibrations (SI. Fig. S1), respectively similar to our earlier report [25,26]. It also shows broad IR bands centered in the range 1305–1450 cm^{-1} due to presence of the nitrate ion [36]. We study room temperature magnetic moment of HmC-3 and the result suggests that it is diamagnetic species as expected for low spin d^6 Co (III) system. The UV–Vis spectrum of HmC-3 is

Table 1
Crystal data and details of the structure determination for HmC-2.

Formula	C20H24FeN3O10
Formula weight	522.27
Crystal system	triclinic
Space group	$P\bar{1}$
a (Å)	9.3895(14)
b (Å)	11.1153(17)
c (Å)	11.1193(17)
α (°)	104.872(2)
β (°)	94.444(2)
γ (°)	95.987(2)
V (Å^3)	1108.9(3)
Z	2
D_{calc} (g cm^{-3})	1.564
μ(Mo Kα) (mm)	0.743
F(000)	542
Crystal size (mm)	0.29 × 0.31 × 0.35
T (K)	293
Radiation (Å)	Mo Kα 0.71073
θ_{min}, θ_{max} (°)	1.9, 25.68
Tot., Uniq. Data, R_{int}	8316, 4143, 0.0279
Observed data ($I > 2\sigma(I)$)	3072
N_{ref}, N_{par}	4143, 325
R, wR_2, *S*	0.0456, 0.1232, 1.051

$w = 1/[s^2(F_o^2) + (0.0572P)^2 + 0.4387P]$, where $P = (F_o^2 + 2F_c^2)/3$.

recorded in different solvents such as DMF, DMSO, acetonitrile, methanol and dichloromethane. All the results are similar enough to suggest about the molecular stability of the complex in all the solutions. Generally in UV–Vis study, low-spin d^6 Co(III) complex displays two visible bands ostensibly associated with the $^1A_{1g} \rightarrow {}^1T_{1g}$ and $^1A_{1g} \rightarrow {}^1T_{2g}$ transitions in octahedral crystal fields [37]. The electronic spectrum for HmC-3 in acetonitrile (SI. Fig. S9) shows a d–d band at 608 nm along with two bands at 410 nm and 324 nm which are attributable to ligand to metal charge transfer (LMCT) transitions [38]. The diamagnetic cobalt complex has allowed a comparison of the solid-state structure with that in solution, as determined by ^1H NMR. Appearance of sharp signals in the NMR spectra is consistent with the expected diamagnetism of the complex. As shown by the ^1H NMR spectrum (SI. Fig. S6) recorded in d^6-DMSO, all the characteristic resonances due to the coordinated Schiff-base ligand appear at expected positions. The simplicity of the spectrum clearly indicates the presence of only one type of environment for ligand and that environment is most likely tetragonally distorted octahedral having pseudo-D_{4h} as is revealed from electronic spectral study (*vide infra*). The NMR and UV–Vis spectral studies thus suggest the retention of the structure on dissolution and the bulk purity of the product. Molar conductance of HmC-3 in acetonitrile medium is 102 Ω^{-1} cm^2 M^{-1} implies that it is 1:1 electrolyte. The cyclic voltammogram of HmC-3 exhibits only one quasireversible redox couple at −0.615/0.130 V, (SI. Fig. S8) indicating that only a single species is present in solution and the observed reduction potential ($E_{1/2}$) is comparable to the earlier reported values for Co(III/II) system [39]. The water content in HmC-3 has been verified by appropriate weight losses in their thermogravimetric (TG) analyses. These weight losses and their corresponding temperatures are noted in experimental section. The ESI-MS study shows the molecular ion peak for HmC-3 at 477.93 amu agree well with the molecular compositions of $[CoL^1{\cdot}2H_2O + CH_3OH]^+$ (SI. Fig. S7). Here it is important to note that the purpose of choosing L^1 as ligand is to utilize its two free aldehyde groups for heterogenization via Schiff-base condensation reaction.

3.2. Description of structure of HmC-2

The structure of HmC-2 has been depicted in Fig. 1. Selected bond lengths and bond angles are listed in Table 2. The complex is six-coordinated and the geometry can be best described as slightly distorted octahedral. The two phenolic O atoms and the two imine N atoms of Schiff-base constitute the basal plane and two O atoms of two water molecules are occupying the axial

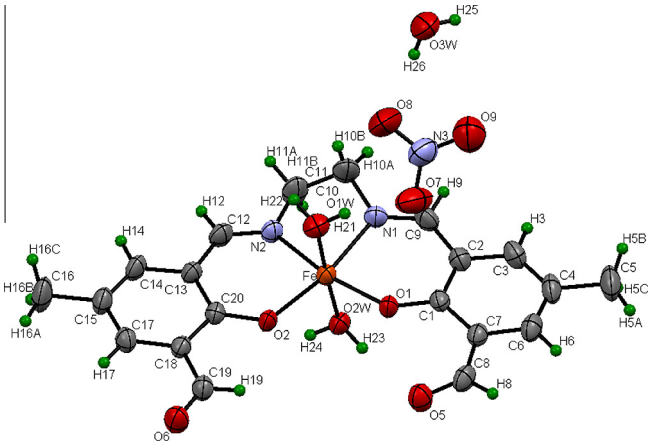

Fig. 1. ORTEP view of HmC-2 with non hydrogen atom labeling scheme having 50% thermal ellipsoid probability.

Table 2
Selected bond lengths (Å) and angles (°) for complex HmC-2.

Fe–01	1.893(2)	O1–Fe–O2W	86.33(9)
Fe–02	1.940(2)	O1–Fe–O2	105.36(9)
Fe–O1W	2.032(3)	O1–Fe–O1W	93.15(10)
Fe–N(2)	2.082(3)	O1–Fe–N1	88.05(10)
Fe–N(1)	2.099(3)	O1–Fe–N2	165.19(10)
Fe–O2W	2.122(2)	O2W–Fe–N1	88.18(10)
C7–C8	1.435(5)	O2–Fe–O2W	90.22(9)
O1–C1	1.315(4)	O1W–Fe–O2W	177.40(10)
O5–C8	1.214(4)	O2W–Fe–N2	87.69(10)
N1–C9	1.274(4)	O2–Fe–N1	166.38(10)
N1–C10	1.466(4)	O1W–Fe–N1	89.25(11)
C1–C2	1.424(4)	N1–Fe–N2	78.23(11)
C1–C7	1.411(4)	O2–Fe–O1W	92.37(10)
		O2–Fe–N2	88.19(10)

positions. Two Fe–O (Phenolic) have slightly different bond distance, 1.893 (2) and 1.940(2) Å respectively, whereas two Fe–N (imine) distances of 2.099(3) and 2.082(3) Å, are comparable. Two Fe–O (H_2O) bond distances are 2.122(2) and 2.032(3) suggesting that HmC-2 has distorted octahedral geometry.

3.3. Preparation and characterization of heterogeneous catalysts

We have prepared 3-aminopropyltrietoxysilane-functionlized, 2D-hexagonally ordered MCM-41 type material and estimated titrimetrically that 5.3% of 3-APTES is introduced into M-II following a published procedure [27]. Thermogravimetric analysis of M-II also strongly support these values (SI. Fig. S12). These results clearly show that 3-aminopropyltriethoxysilane (3-APTES) has been attached into M-I. Heterogenization of all the homogenous catalysts (HmC-1, -2 and -3) are carried out following the similar method as described in experimental section. The UV–Vis study of heterogenized catalysts (HtC-1, -2 and -3) in solid state show four absorption peaks in the range of 250–450 nm similar to earlier report [27] along with a broad band for d–d transition in the range of 500–800 nm. (SI. Fig. S13) Infrared spectroscopy has been used extensively for the characterization of M-II and all the heterogeneous catalysts (HtC-1, -2 and -3) (SI. Figs. S2–S5). Water of hydration usually exhibits one strong sharp band near 3500 cm^{-1}. In addition, the rocking motion of bridging oxygen perpendicular to the Si–O–Si plane can be correlated with the 445 cm^{-1} band which is common to all the spectra. The substitution of silicon 3-APTES causes shifts of the lattice vibration bands to lower wave numbers. The wave numbers of anti-symmetric Si–O–Si vibration band of M-II, HtC-1, HtC-2 and HtC-3 decreases to the region of 1090–1095 cm^{-1}. FTIR spectra of M-II, HtC-1, HtC-2 and HtC-3 also suggest the presence of various N–H and C–H vibration bands in the 3500–2800 cm^{-1} and 1650–1500 cm^{-1} respectively. The free aldehyde group of 2, 6-diformyl-4-methylphenol shows a band at ~1655–1665 cm^{-1} in the FTIR spectrum of (HmC-1, -2 and -3), but no such band has been detected in the spectra of heterogenized catalysts (HtC-1, -2 and -3). Rather, C=N and C=C stretching frequency appear in the region of 1630–1650 cm^{-1} and 1542–1548 cm^{-1} respectively for all the heterogenized catalysts. Sharp band in the 1382–1388 cm^{-1} region suggest the presence of NO_3^- in HtC-2 and HtC-3. Thus, it is confirmed that both free aldehyde groups of homogenous catalysts (HmC-1, -2 and -3) are converted into Schiff bases. We also performed the powder X-ray diffraction of M-II and all the heterogeneous catalysts (HtC-1, -2 and -3). The small angle diffraction peaks of M-II appeared at very similar position as previous reported [27]. Similarity of the diffraction patterns of M-II, HtC-1, HtC-2 and HtC-3 indicates that the 2D hexagonal ordering has been retained after addition of Schiff-base complex with M-II. Only an overall decrease in intensity of peaks is

observed (SI. Fig. S10). This is recognized to the lowering of local order as stated previously by Lim and Stein [40]. We also studied the morphology of heterogenized complexes (HtC-1, -2 and -3). Scanning electron micrographs of M-II, HtC-1, HtC-2 and HtC-3 are shown in Fig. 2. Introduction of Mn(III), Fe(III) and Co(III) Schiff base complexes into M-II influenced the morphology of the mesoporous material. Compare to M-II, all heterogeneous catalysts exhibit smaller particle size which is supposed to be due to complexation. On passing from HtC-1 to HtC-3, the particle size is observed to decrease and aggregation of particle is increased significantly. The smallest particle size and the most symmetric distribution of HtC-3 particles suggests that maximum complexation takes place in this case and after complexation the complex aggregated or agglomerated into smaller sized clusters over the entire surface of M-II.

We have estimated titrimetrically the amount of 3-APTES which have been introduced into M-II (Table 3). Thermogravimetric analysis of M-II also strongly supports this value (SI. Fig. S12). In HtC-1, HtC-2 and HtC-3, –OH (phenolic) groups are converted into $-O^{--}M^{n+}$ [M = Mn, Fe, Co, $n = 3$] salt. Therefore to understand the amount of Schiff-base complexes (HtC-1, HtC-2 and HtC-3) formed in M-III, we only performed thermogravimetric analysis of them. Thermogravimetric results of (HtC-1, -2 and -3) along with (HmC-1, -2 and -3) show that 12.56%, 12.34% and 12.58% Schiff-base complexes are loaded in their heterogenised form. (SI. Figs. S11–12) All the results are shown in Table 3.

Table 3
The loading of functional groups in the materials as estimated by different method.

Loading (wt%)	Method	
	Titration	Thermogravimetry
3-APTES in M-II	5.50	5.60
HmC-1 in HtC-1	–	12.56
HmC-2 in HtC-2	–	12.34
HmC-3 in HtC-3	–	12.58

3.4. Catalytic epoxidation of alkenes by homogenous catalysts

The same procedure has been followed to study the epoxidation reaction catalyzed by three homogeneous catalysts, HmC-(1-3). In a typical reaction, (*E*)-stilbene (540 mg, 3 mmol) (as representative), catalyst (0.1 mmol), 70% TBHP (540 mg, 6 mmol) or PhIO (666 mg, 3 mmol) were mixed in 50 mL dichloromethane/acetonitrile and stirred for 2 h at room temperature. The progress of the reaction was monitored by TLC. After usual work up and chromatographic purification, the isolated yield of epoxide was found to be 84% and 83% for terminal oxidant TBHP and PhIO respectively when acetonitrile used as a solvent. Whereas the yield was 82% and 80% when dichloromethane used as a solvent. Before to precede further optimization of the catalysis conditions *viz* amount of catalyst, time and amount of terminal oxidant required to obtaining the maximum epoxide yield, has been determined. To optimize the catalyst requirement, catalyst concentration (considering HmC-3) was varied between 40 and 60 mg per 3 mmol of (*E*)-stilbene. Increase in the yield of epoxide was observed when the amount of catalyst was increased from 40 to 50 mg but the yield remained same with further increment of catalyst amount up to 60 mg. Then the reaction was studied with varying amounts of TBHP or PhIO. The yield of the epoxide also increases with increasing the concentration of the oxidant, TBHP or PhIO. This catalytic reaction was also examined with varying the time period between 1 and 3 h where we observed the epoxide yield attained the peak after 2hr of reaction and remained the same even after 3hr. An optimum of 50 mg (~0.1mmnol) of catalyst, 70% TBHP (450 mg, 5 mmol) or PhIO (666 mg, 3 mmol) (per 3 mmol of the substrate) and 2hr reaction time are ideal for achieving the best yield. Table 4 represents the (*E*)-stilbene epoxide yields under different conditions using HmC-3 as catalyst.

However, the optimum reaction conditions thus determined have been followed in HmC-1 and HmC-2 catalyzed epoxidation reactions. The essential role played by the catalyst is evident from the extremely low (<2%) yield of epoxide found in a blank reaction carried out in absence of the catalyst.

3.4.1. Epoxidation with PhIO or TBHP

We earlier studied HmC-1 and the ClO_4^- analogue of HmC-2 as epoxidation catalyst using (*E*)-stilbene and styrene as substrates and PhIO as terminal oxidant [25,26]. So here we studied only HmC-3 catalyzed epoxidation with PhIO and HmC-1, -2 and -3 catalyzed epoxidation of (*E*)-stilbene or styrene in CH_3CN or CH_2Cl_2 with TBHP (Table 5). We found 83% and 81% epoxide yield for (*E*)-stilbene epoxidation, 62% and 59% epoxide yield for styrene epoxidation, 79% and 78% epoxide yield for cyclooctene epoxidation and 77% and 76% epoxide yield for 1-octene epoxidation in CH_2Cl_2 and CH_3CN respectively, catalyzed by HmC-3 in presence of PhIO. When we used TBHP as terminal oxidant and HmC-1, -2 and -3 as catalyst, epoxide yield ranges from 88–55% in CH_3CN and 87–50% in CH_2Cl_2 for (*E*)-stilbene epoxidation and in case of styrene epoxidation, the isolated epoxide yield ranges from 75–54% in CH_3CN and 73–43% in CH_2Cl_2. For cyclooctene epoxidation ranges from 81–55% in CH_3CN and 80–49% in CH_2Cl_2. When substrate is 1-octene the ranges are 85–56% in CH_3CN and 80–53% in CH_2Cl_2. (Table 5)

3.5. Epoxidation of alkenes by heterogeneous catalysts

Here also first of all we evaluate the optimum reaction conditions to achieve the maximum epoxide yield as we have performed in homogeneous system. For this purpose the weight of heterogeneous catalysts (HtC-1 or -2 or -3) were varied between 100 and

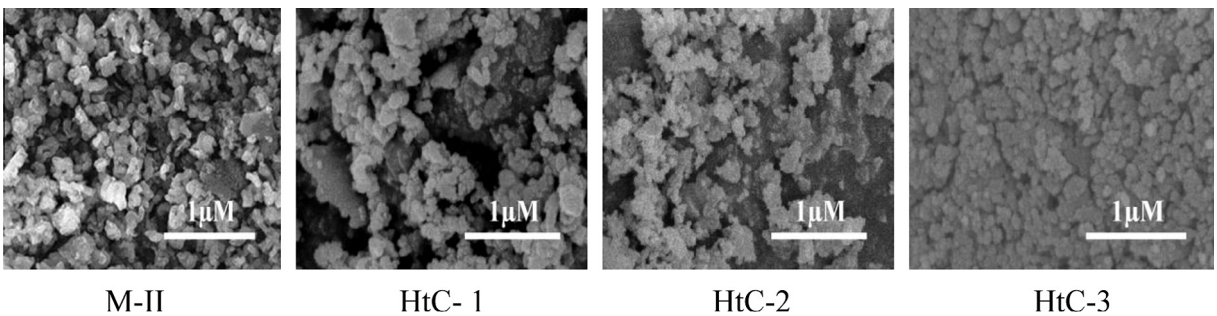

Fig. 2. Scanning electron micrographs of M-II, HtC-1, HtC-2 and HtC-3.

Table 4
Catalytic epoxidation of (*E*)-stilbene in CH_3CN and CH_2Cl_2 by TBHP or PhIO using HmC-3 as the catalyst under different conditions.

Entry	Catalyst (mg)	Solvent	TBHP (mmol)	PhIO (mmol)	Time (h)	Conversion (%)	TON[a]	Yield (%)[b]
1	40	CH_3CN	5	–	2	60	21	56
		CH_2Cl_2				55	18	49
2	45	CH_3CN	5	–	2	83	26	81
		CH_2Cl_2				80	26	79
3	50	CH_3CN	5	–	2	90	26	84
		CH_2Cl_2				86	25	82
4	60	CH_3CN	5	–	2	91	22	86
		CH_2Cl_2				86	21	82
5	40	CH_3CN	–	3	2	53	18	49
		CH_2Cl_2				50	15	41
6	45	CH_3CN	–	3	2	80	26	79
		CH_2Cl_2				78	26	76
7	50	CH_3CN	–	3	2	88	25	83
		CH_2Cl_2				85	24	81
8	60	CH_3CN	–	3	2	89	21	84
		CH_2Cl_2				87	20	80
9	50	CH_3CN	3	–	2	50	15	48
		CH_2Cl_2				46	12	41
10	50	CH_3CN	8	–	2	91	26	85
		CH_2Cl_2				89	25	82
11	50	CH_3CN	–	2	2	48	12	40
		CH_2Cl_2				46	12	39
12	50	CH_3CN	–	4	2	90	25	82
		CH_2Cl_2				86	25	82

[a] TON = moles of substrate converted per mole of catalyst.
[b] Isolated epoxide yield.

Table 5
Epoxidation of (*E*)-stilbene and styrene catalyzed by HmC-1, -2 and -3 in CH_3CN or CH_2Cl_2 with different terminal oxidants.

Catalyst	Substrate	Solvent	Conversion (%)		TON[a]		Yield (%)[b]	
			TBHP	PhIO	TBHP[c]	PhIO[d]	TBHP[c]	PhIO[d]
HmC-1	(*E*)-stilbene	CH_3CN	97	93	27	26	88	86
		CH_2Cl_2	93	89	26	25	87	83
	styrene	CH_3CN	78	76	23	19	75	63
		CH_2Cl_2	76	75	22	18	73	60
	cyclooctene	CH_3CN	86	84	25	24	81	79
		CH_2Cl_2	84	76	24	22	80	75
	1-octene	CH_3CN	89	88	26	24	85	82
		CH_2Cl_2	84	80	24	23	80	77
HmC-2	(*E*)-stilbene	CH_3CN	56	51	17	14	55	47
		CH_2Cl_2	55	49	15	13	50	43
	styrene	CH_3CN	55	54	16	14	54	47
		CH_2Cl_2	51	49	13	12	43	40
	cyclooctene	CH_3CN	55	55	17	16	55	54
		CH_2Cl_2	53	59	15	16	49	53
	1-octene	CH_3CN	56	55	17	16	56	54
		CH_2Cl_2	54	53	16	16	53	53
HmC-3	(*E*)-stilbene	CH_3CN	90	88	26	25	84	83
		CH_2Cl_2	86	85	25	24	82	81
	styrene	CH_3CN	77	76	23	19	75	62
		CH_2Cl_2	73	72	21	18	71	59
	cyclooctene	CH_3CN	81	84	24	23	80	79
		CH_2Cl_2	80	80	24	23	80	78
	1-octene	CH_3CN	82	81	25	23	81	77
		CH_2Cl_2	79	78	24	23	79	76

[a] TON = moles of substrate converted per mole of catalyst.
[b] Isolated epoxide yield.
[c] Catalyst (0.1 mmol), alkenes (3 mmol), 70% TBHP (450 mg, 5 mmol) and CH_3CN or CH_2Cl_2 (50 ml), were stirred at room temperature for 2 h in air.
[d] Catalyst (0.1 mmol), alkenes (3 mmol), PhIO (666 mg, 3 mmol), and CH_3CN or CH_2Cl_2 (50 ml), were stirred at room temperature for 2 h in air.

400 mg for per 3 mmol of styrene. Increase in the yield of epoxide was observed when the amount of catalyst was increased from 100 to 200 mg but the yield remained same with further increment of catalyst amount up to 400 mg. The reaction was also studied with varying the amounts of terminal oxidant, TBHP or PhIO and the time. The results showed that 70% TBHP (360 mg, 4 mmol) or PhIO (660 mg, 3 mmol) and 2 h time is good for epoxidation study. At the end of the reaction, the catalyst was filtered and reused for

further epoxidation. Here it is noteworthy that we did not find any leaching of catalysts during the epoxidation reaction.

3.5.1. Epoxidation with PhIO or TBHP

Table 6 shows the maximum isolated yield (%) for HtC-1, -2 and -3 catalyzed epoxidation of four different alkenes, using PhIO or TBHP as terminal oxidants in CH_3CN and CH_2Cl_2. When we used PhIO as terminal oxidant, we observed the isolated epoxide yield ranges from 84–55% in CH_3CN and 83–52% in CH_2Cl_2 for (*E*)-stilbene epoxidation, 75–49% in CH_3CN and 72–47% in CH_2Cl_2 for styrene epoxidation, 80–54% in CH_3CN and 78-59% in CH_2Cl_2 for Cyclooctene epoxidation and the ranges are 79–55% in CH_3CN and 73–53% in CH_2Cl_2 for 1-octene epoxidation (see Table 6). But when we used TBHP as terminal oxidant, we observed the isolated epoxide yield ranges from 85–56% in CH_3CN and 84–54% in CH_2Cl_2 for (*E*)-stilbene epoxidation, whereas the isolated epoxide yield ranges from 75–52% in CH_3CN and 76–50% in CH_2Cl_2 for styrene epoxidation, 80–55% in CH_3CN and 81–55% in CH_2Cl_2 for cyclooctene epoxidation and the ranges are 83–60% in CH_3CN and 79–59% in CH_2Cl_2 for 1-octene epoxidation (see Table 6).

3.6. Probable reaction pathways

It is already well documented that the mechanistic pathways in expoxidation employing PhIO and TBHP as terminal oxidants are totally different (Scheme 2). When PhIO is used as terminal oxidant it is believed that initially higher valent metal-oxo species is formed as the active intermediate followed by oxo transfer to the olefinic double band to form epoxide [25,26,41–45]. On the other hand, when TBHP is used as the terminal oxidant, the reaction is supposed to proceed via radical pathway [42]. Previously we detected, when PhIO was added to the catalyst the color started fading as a consequence of the formation higher valent metal-oxo species and when complete consumption of PhIO took place, the intensity of the color turned back nearly to the original intensity, indicating the catalyst regeneration [25]. Here we also have got the same observation with HmC-3. (SI. Fig. S9) But in case of TBHP no such incident is happened which implies that in presence of TBHP as terminal oxidant no higher valent metal-oxo species is generated as the active intermediate. However, on comparing Tables 5 and 6 it may be stated that in our both homogeneous and heterogeneous systems higher epoxide yields are obtained with TBHP as terminal oxidant. Amongst the homogeneous catalysts Mn-system shows the highest activity followed by Co- and Fe-system. One the contrary, amongst the heterogeneous systems Co-system shows higher efficiency followed by Mn- and Fe-system. The lower activity of the homogeneous Co- and Fe-systems when PhIO acts as terminal oxidant is supposed to be due to the formation of dimeric or polymeric μ-oxo species which are inactive to transfer the oxo group to olefinic double bond. On the other hand, the very good activity of Mn-system implies that the deactivating dimeric or polymeric μ-oxo species generation is not facilitating here. It is well documented [41,46] that dimeric μ-oxo-Mn(IV) species, if formed, are in equilibrium with active oxomangenese(V) species and in presence of active olefins as we used for our present study, the equilibrium shifted towards oxomangenese(V) species. The high activity of heterogeneous Co-system suggests that on heterogenization higher valent Cobalt-μ-oxo species formation facilitate. On heterogenization the silica based solid support present at the close vicinity of metal centers prevents the generation of inactive di-/polymeric μ-oxo species obviously due to steric effect in all cases and it becomes the most prominent in case of HtC-3 which has the smallest Co(III).

3.7. Reusability of the heterogeneous catalysts

We have studied the recycling efficiency of the heterogeneous catalysts (HtC-1, HtC-2 and HtC-3) i.e. whether the catalysts can

Table 6
Epoxidation of (*E*)-stilbene and styrene catalyzed by HtC-1, -2 and -3 in CH_3CN or CH_2Cl_2 with different terminal oxidants.

Catalyst	Substrate	Solvent	Conversion (%)		TON[a]		Yield (%) [b]	
			TBHP	PhIO	TBHP[c]	PhIO[d]	TBHP[c]	PhIO[d]
HtC-1	(*E*)-stilbene	CH_3CN	82	78	42	39	78	73
		CH_2Cl_2	72	70	38	37	71	69
	styrene	CH_3CN	69	68	35	34	65	64
		CH_2Cl_2	68	66	32	31	59	58
	cyclooctene	CH_3CN	76	74	38	36	71	68
		CH_2Cl_2	72	68	38	35	70	66
	1-octene	CH_3CN	80	77	43	40	80	75
		CH_2Cl_2	75	71	40	38	75	71
HtC-2	(*E*)-stilbene	CH_3CN	60	58	35	34	56	55
		CH_2Cl_2	59	57	34	32	54	52
	styrene	CH_3CN	55	53	33	30	52	49
		CH_2Cl_2	53	52	31	29	50	47
	cyclooctene	CH_3CN	58	56	35	33	55	54
		CH_2Cl_2	56	61	34	36	55	59
	1-octene	CH_3CN	60	59	38	36	60	58
		CH_2Cl_2	59	53	37	33	59	53
HtC-3	(*E*)-stilbene	CH_3CN	89	87	56	54	85	84
		CH_2Cl_2	87	85	55	54	84	83
	styrene	CH_3CN	80	76	51	49	78	75
		CH_2Cl_2	79	75	49	47	76	72
	cyclooctene	CH_3CN	80	81	52	52	80	80
		CH_2Cl_2	81	80	53	51	81	78
	1-octene	CH_3CN	83	82	54	51	83	79
		CH_2Cl_2	81	79	52	50	79	77

[a] TON = moles of substrate converted per mole of catalyst.
[b] Isolated epoxide yield.
[c] Catalyst (200 mg), alkenes (3 mmol), 70% TBHP (360 mg, 4 mmol) and CH_3CN or CH_2Cl_2 (50 ml), were stirred at room temperature for 2 h in air.
[d] Catalyst (200 mg), alkenes (3 mmol), PhIO (666 mg, 3 mmol), and CH_3CN or CH_2Cl_2 (50 ml), were stirred at room temperature for 2 h in air.

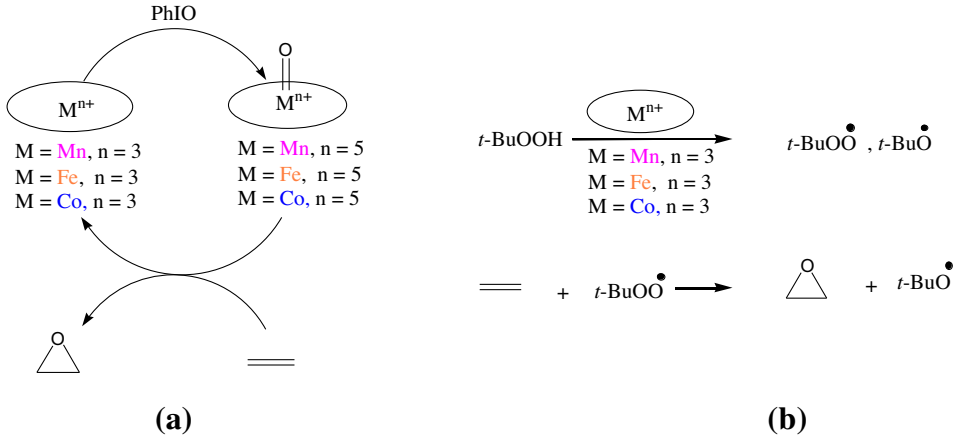

Scheme 2. Probable mechanism for the catalytic epoxidation in presence of (a) PhIO as terminal oxidant and (b) TBHP as terminal oxidant.

Table 7
Reuse of HtC-1, HtC-2 and HtC-3 with TBHP and PhIO for epoxidation of (*E*)-stilbene in CH_3CN.

Catalyst	Catalyst (mmol%)[a]	TBHP (mmol)	PhIO (mmol)	Time (hr)	Yield (%)[b]									
					TBHP					PhIO				
Reused number ⇒					1	2	3	4	5	1	2	3	4	5
HtC-1	0.028	4	3	2	78	78	77	76	76	73	72	71	71	70
HtC-2	0.024	4	3	2	56	55	54	54	53	55	54	54	54	53
HtC-3	0.023	4	3	2	85	85	85	84	84	84	83	83	82	82

[a] mmol of homogeneous counterpart per 100 mg of heterogeneous catalyst.
[b] Isolated yield of epoxide.

be reused further for several cycles. (*E*)-Stilbene has been chosen as a representative case for recycling experiments. After each reaction cycle the catalysts were recovered by filtration, washed thoroughly with acetonitrile and then treated with 0.1 M HCl or HNO_3 solution in methanol at 50 °C for 5 h depending on the presence of counter anion in catalysts for their regeneration. Finally they were dried at 100 °C for 2 h. The catalytic reactions have been carried out following the same experimental procedure as that with the original catalysts. For all cases, the yields of the catalytic reactions were not significantly different through first to fifth use (Table 7). It is important to mention that the morphology of HtC-1, HtC-2 and HtC-3 do not change after epoxidation reaction which probably the key factor for its reusable property.

4. Conclusion

We, here demonstrate a simple and smart technique to heterogenize structurally characterized efficient homogeneous epoxidation catalysts based on Schiff-base complexes via immobilizing on MCM-41 surface. The unique feature of these heterogeneous catalysts is that the active site metal coordination sphere is structurally assigned. The catalytic activity of Co-complex as homogeneous expoxidation catalyst has been thoroughly investigated and reported here, whereas similar study with its Fe and Mn counterpart were reported earlier. Schiff-base condensation between aldehydic part of those three Schiff-base complexes and the pending primary amine of MCM-41 is basis of the heterogenization process. The heterogeneous catalysts thus obtained, namely HtC-1 to 3 have been thoroughly explored as expoxidation catalysts. As substrate (*E*)-stilbene, styrene, cyclooctene, 1-octene and as terminal oxidant TBHP and PhIO have been employed. Per cycle activity wise all three heterogeneous catalysts are less efficient in compare to their homogeneous counterpart. However, since our heterogeneous catalysts are very robust, no leaching is observed during catalytic reaction and can be used several times just after simple filtration, the overall activity of these three heterogeneous catalysts are far better than their respective homogeneous counterpart. Amongst the three homogeneous catalysts Mn catalyst shows the highest efficiency followed by Co and Fe counterparts. On the contrary, after heterogenization the Co-based catalyst exhibits the highest performance.

Acknowledgements

The authors wish to thank CSIR, New Delhi [CSIR project No. 01(2464)/11/EMR-II dated 16-05-2011] for financial support. We also thank Department of Science and Technology (DST), New Delhi, for providing single crystal diffractometer facility at the Department of Chemistry, University of Calcutta, through DST-FIST program. Authors are thankful to Professor Ennio Zangrando, Dipartimento di Scienze Chimiche e Farmaceutiche, University of Trieste, Trieste, Italy for his generous help for final solution of the crystal structure.

Appendix A. Supplementary material

CCDC 884978 contains the supplementary crystallographic data for HmC-2. These data can be obtained free of charge from The Cambridge Crystallographic Data Centre via www.ccdc.cam.ac.uk/data_request/cif. Supplementary data associated with this article can be found, in the online version, at http://dx.doi.org/10.1016/j.ica.2013.06.045.

References

[1] For recent advances, see R.A. Sheldon (Ed.), J. Mol. Catal. A 117 (1997) 1.
[2] H. Yoon, T.R. Wagler, K.J. O'Connor, C.J. Burrows, J. Am. Chem. Soc. 112 (1990) 4568.

[3] X.-H. Lu, Q.-H. Xia, H.-J. Zhan, H.-X. Yuan, C.-P. Ye, K.-X. Su, G. Xu, J. Mol. Catal. A: Chem. 250 (2006) 62.
[4] L. Gomez, I. Garcia-Bosch, A. Company, Sala, X. Fontrodona, X. Ribas, M. Costas, J. Chem. Soc., Dalton Trans. 47 (2007) 5539.
[5] C. Coperet, M. Chabanas, R.P. Saint-Arroman, J.M. Basset, Angew. Chem., Int. Ed. Engl. 42 (2003) 156.
[6] N. Mizuno, M. Misono, Chem. Rev. 98 (1998) 199.
[7] F. Lefebvre, J.M. Basset, J. Mol. Catal. A: Chem. 146 (1999) 3.
[8] D. Brunel, N. Bellocq, P. Sutra, A. Cauvel, M. Laspéras, P. Moreau, F.D. Renzo, A. Galarneau, F. Fajula, Coord. Chem. Rev. 178–180 (1998) 1085.
[9] J.Y. Ying, C.P. Mehnert, M.S. Wong, Angew. Chem., Int. Ed. Engl. 38 (1999) 56.
[10] A. Choplin, F. Quignard, Coord. Chem. Rev. 178–180 (1998) 1679.
[11] D.R. Leanord, J.R. Lindsay Smith, J. Chem. Soc, Perkin Trans. 2 (1) (1991) 25.
[12] I.F.J. Vankelecom, D. Tas, R.F. Parton, Vyver. VVde, P.A. Jacobs, Angew. Chem., Int. Ed. Engl. 35 (1996) 1346.
[13] G. Xiang, Zhou, X.Q. Yu, J.S. Huang, S.G. Li, L.S. Lib, C.M. Che, Chem. Commun. 18 (1999) 1789.
[14] P.K. Saha, S. Saha, S. Koner, J. Mol. Catal. A: Chem. 203 (2003) 173.
[15] T. Chattopadhyay, M. Kogiso, M. Aoyagi, H. Yui, M. Asakawa, T. Shimizu, Green Chem. 13 (2011) 1138.
[16] B.B. De, B.B. Lohray, S. Sivaram, P.K. Dhal, Tetrahedron Asymmetry 6 (1995) 2105.
[17] F. Minutolo, D. Pini, A. Petri, P. Salvadori, Tetrahedron Asymmetry 7 (1996) 2293.
[18] M.J. Sabater, A. Corma, A. Domenech, V. Fornés, H. García, Chem. Commun. 14 (1997) 1285.
[19] P. Piaggio, P. McMorn, C. Langham, D. Bethell, P.C. Bulman-Page, F.E. Hancock, G.J. Hutchings, New J. Chem. 22 (1998) 1167.
[20] S.B. Ogunwumi, T. Bein, Chem. Commun. 9 (1997) 901.
[21] Q. Zhang, Y. Wang, S. Itsuki, T. Shishido, K. Takehira, J. Mol. Catal. A: Chem. 188 (2002) 189.
[22] M. Masteri-Farahani, F. Farzaneh, M. Ghandi, J. Mol. Catal. A: Chem. 248 (2006) 53.
[23] S. Jana, B. Dutta, R. Bera, S. Koner, Langmuir 23 (2007) 2492.
[24] M. Nandi, P. Roy, H. Uyama, A. Bhaumik, J. Chem. Soc., Dalton Trans. 40 (2011) 12510.
[25] D. Das, C.P. Cheng, J. Chem. Soc., Dalton Trans. 7 (2000) 1081.
[26] T. Chattopadhyay, D. Das, J. Coord. Chem. 5 (2009) 845.
[27] K. Sarkar, K. Dhara, M. Nandi, P. Roy, A. Bhaumik, P. Banerjee, Adv. Funct. Mater. 19 (2009) 223.
[28] R.R. Gagne, C.L. Spiro, T.J. Smith, C.A. Hamann, W.R. Thies, A.K. Shiemeke, J. Am. Chem. Soc. 103 (1981) 4073.
[29] H. Saltzman, J.G. Sharefkin, Org. Synth. Colloid 5 (1973) 658.
[30] Bruker, SMART, SAINT, Software Reference Manual Bruker AXS Inc. Madison, Wisconsin, USA, 2000.
[31] G.M. Sheldrick, Acta. Crystallogr., Sect A. 64 (2008) 112.
[32] G.M. Sheldrick, SHELXL 97, Program for the Refinement of Crystal Structures, University of Gottingen, Germany, 1997.
[33] L.J. Farrugia, J. Appl. Crystallogr. 32 (1999) 837.
[34] A.L. Spek, PLATON, Molecular Geometry Program, University of Utrecht, The Netherlands, 1999.
[35] L.J. Farrugia, J. Appl. Crytallogr. 30 (1997) 565.
[36] K. Nakamoto, Infrared and Raman Spectra of Inorganic and Coordination Compounds, third ed., Wiley, New York, 1978.
[37] G.P. Marianne, P.S. Kenneth, J.C. Carl, Inorg. Chem. 21 (1982) 2972.
[38] B.N. Figgis, M.A. Hitchman, Ligand Field Theory and its Applications, Wiley–VCH, USA, 2000.
[39] D.F. Averill, R.F. Broman, Inorg. Chem. 17 (1978) 3389.
[40] M.H. Lim, A. Stein, Chem. Mater. 11 (1999) 3285.
[41] K. Srinivasan, P. Michaud, J.K. Kochi, J. Am. Chem. Soc. 108 (1986) 2309.
[42] J.D. Koola, J.K. Kochi, J. Org. Chem. 52 (1987) 4545.
[43] W. Zhang, J.L. Loebach, S.R. Wilson, E.N. Jacobsen, J. Am. Chem. Soc. 112 (1990) 2801.
[44] T. Katsuki, J. Mol. Catal. A: Chem. 113 (1996) 87.
[45] C. Linde, M. Arnold, P.O. Norrby, B. Akermark, Angew. Chem., Int. Ed. Engl. 36 (1997) 1723.
[46] P.K. Dhal, B.B. De, S. Sivaram, J. Mol. Catal. A: Chem. 177 (2001) 71.